



# Canadian Journal of Chemistry

## Effect of hydrogen-bond strength on photoresponsive properties of polymer-azobenzene complexes

Journal:	<i>Canadian Journal of Chemistry</i>
Manuscript ID	cjc-2020-0048.R1
Manuscript Type:	Article
Date Submitted by the Author:	26-Mar-2020
Complete List of Authors:	Vapaavuori, Jaana; Université de Montréal, Département de chimie; Aalto University, School of Chemical Engineering Koskela, Jenni; Aalto University, Department of Applied Physics Wang, Xiaoxiao; Université de Montréal, Département de chimie Ras, Robin; Aalto University, Department of Applied Physics; Aalto University, Department of Bioproducts and Biosystems Priimagi, Arri; Tampere University, Faculty of Engineering and Natural Sciences Bazuin, C. Geraldine; Université de Montreal Pellerin, Christian; Université de Montréal, Département de chimie
Is the invited manuscript for consideration in a Special Issue?:	University of Montreal
Keyword:	supramolecular complexes, azo-containing materials, photo-orientation, surface relief gratings

SCHOLARONE™  
Manuscripts

## Effect of hydrogen-bond strength on photoresponsive properties of polymer-azobenzene complexes

Jaana Vapaavuori<sup>a,#,\*</sup>, Jenni E. Koskela<sup>b</sup>, Xiaoxiao Wang<sup>a</sup>, Robin H. A. Ras<sup>b,c</sup>, Arri Priimagi<sup>d</sup>, C. Geraldine Bazuin<sup>a,\*</sup>, Christian Pellerin<sup>a,\*</sup>

- a. Département de chimie, Université de Montréal, C.P. 6128, Succ. Centre-Ville, Montréal, QC, Canada H3C 3J7
  - b. Department of Applied Physics, Aalto University School of Science, Puumiehenkuja 2, 02150 Espoo, Finland
  - c. Department of Bioproducts and Biosystems, Aalto University School of Chemical Engineering, Kemistintie 1, 02150 Espoo
  - d. Smart Photonic Materials, Faculty of Engineering and Natural Sciences, Tampere University, P.O. Box 541, 33101 Tampere, Finland
- # Current address: Aalto University, School of Chemical Engineering, Kemistintie 1, 02150 Espoo, Finland
- E-mail addresses of corresponding authors: jaana.vapaavuori@aalto.fi; geraldine.bazuin@umontreal.ca; c.pellerin@umontreal.ca

**Abstract:** Supramolecular complexation between photoresponsive azobenzene chromophores and a photopassive polymer host offers synthetic and design advantages compared to conventional covalent azo-containing polymers. In this context, it is important to understand the impact of the strength of the supramolecular interaction on the optical response. Herein, we study the effect of hydrogen-bonding strength between a photopassive polymer host [poly(4-vinylpyridine), or P4VP)] and three azobenzene analogues capable of forming weaker (hydroxyl), stronger (carboxylic acid), or no H-bonding with P4VP. The hydroxyl-functionalized azo forms complete H-bonding complexation up to equimolar ratio with VP, while the COOH-functionalized azo reaches only up to 30% H-bond complexation due to competing acid dimerization that leads to partial phase separation and azo crystallization. We show that the stronger azo-polymer H-bonding nevertheless provides higher photoinduced orientation and better performance during optical surface patterning, in terms of grating depth and diffraction efficiency, when phase separation is either avoided altogether or is limited by using relatively low azo contents. These results demonstrate the importance of the H-bonding strength on the photoresponse of azopolymer complexes as well as the need to take into account the interplay between different intermolecular interactions that can affect complexation.

**Key words:** supramolecular complexes, azo-containing materials, photo-orientation, surface relief gratings

## Introduction

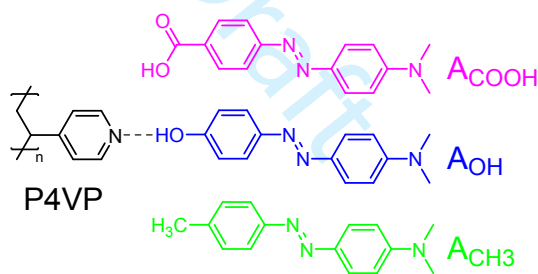
Supramolecular chemistry, based on specific noncovalent interactions between complementary molecules, is an excellent tool for building libraries of functional materials, since with little effort one structural material element at a time can be varied.<sup>1-5</sup> This strategy has been utilized, for instance, for establishing structure-property relationships in polymer-azobenzene complexes.<sup>6-14</sup> These complexes, and azo-containing amorphous materials in general, can convert incident light energy directly into motion, leading to photoinduced dichroism and birefringence as well as to the formation of topological surface patterns such as surface-relief gratings (SRGs) by exposure to interference patterns of light.<sup>15-22</sup>

Since supramolecular materials design relies on spontaneously forming intermolecular physical interactions, it is important to understand the effect of the supramolecular interaction strength on the optical phenomena. To date, there have been relatively few such investigations in polymer-azobenzene complexes. Notably, for halogen-bonding interactions, the non-linear optical response of liquid crystals<sup>23</sup> as well as the photo-orientation<sup>24</sup> and all-optical surface patterning efficiency<sup>25</sup> have been observed to correlate with halogen-bonding strength. Similarly, a comparison between analogous material systems consisting of hydrogen bonding, ionic bonding and mixed hydrogen and ionic bonding<sup>26</sup> demonstrated a dependence of the optical surface patterning efficiency on the type of supramolecular bonding, and thus presumably their strength.

As a natural corollary and given that hydrogen (H) bonding is the most commonly used supramolecular interaction, it is of interest to examine if there is a similar relationship between H-bond strength and optical responses in H-bonded azomaterials. Thus, in this study, we investigate a small library consisting of poly(4-vinylpyridine) (P4VP) as the H-bond acceptor polymer host and two H-bond donor chromophores ( $A_{\text{COOH}}$  and  $A_{\text{OH}}$ , A denoting the azo derivative and COOH

and OH the H-bond donating head groups) over a range of  $A_{\text{head}}:\text{VP}$  molar ratios ( $x = 0.05\text{-}1.0$ ), where the H-bonds of  $A_{\text{COOH}}$  and  $A_{\text{OH}}$  with P4VP are considered to be strong and medium-strength, respectively.<sup>27,28</sup> For comparison, a chromophore with a methyl head group ( $A_{\text{CH}_3}$ ), which has no specific functional group interactions with P4VP, is also studied. The molecular structures and nomenclature of the components are given in Scheme 1. Infrared spectroscopy, UV-visible spectroscopy and polarized optical microscopy are used to characterize the degree of complexation and optical properties of the materials. We then compare the photoresponse of the three systems in terms of photo-orientation upon illumination with linearly polarized light and of SRG depth and diffraction efficiency upon irradiation with an interference pattern of light.

**Scheme 1.** Chemical structures and nomenclature of the polymer and chromophores used.



## Results and discussion

First, the extent of H-bonded pyridine units in the  $\text{P4VP}(A_{\text{OH}})_x$  and  $\text{P4VP}(A_{\text{COOH}})_x$  complexes [not  $\text{P4VP}(A_{\text{CH}_3})_x$  since these have no H-bonding interactions] as a function of azo content was determined by infrared spectroscopy following the methodology established in our previous work.<sup>8</sup> The results in Fig. 1 demonstrate that the degree of H-bonding in the  $\text{P4VP}(A_{\text{OH}})_x$  complexes reaches the nominal values indicated by the  $A_{\text{head}}:\text{VP}$  molar ratios used in the sample preparation, such that a claim of essentially complete H-bonding between  $A_{\text{OH}}$  and P4VP can be made. On the other hand, the  $\text{P4VP}(A_{\text{COOH}})_x$  complexes depart from this trend already at  $x = 0.25$ ,

where the measured degree of H-bonding is less than half the nominal value and never exceeds 30% up to the nominal equimolar ratio. The low degree of H-bonding with P4VP can be related to competing interactions, notably among the COOH groups, which are highly subject to dimerization.<sup>29,30</sup> As will be shown below, this incomplete H-bonding favours phase separation in the P4VP(A<sub>COOH</sub>)<sub>x</sub> system and thus affects the optical clarity of the thin films. Nevertheless, despite this difference in the degree of H-bonding between the two chromophores with P4VP for  $x = 0.25$  and above, it is possible to compare the effect of the H-bond strength on photo-orientation and SRG inscription for at least  $x = 0.05$  and  $0.10$ , for which H-bonding with P4VP is complete in both sets of complexes, keeping in mind also that it has been shown that A<sub>OH</sub> concentrations as low as  $x=0.01$  are enough for photoinduced surface patterning.<sup>31</sup> In addition, it is of interest to examine, for comparison, the consequences of partial H-bonding on the optical properties at high degrees of complexation. It is also worth mentioning here that spin-coating, which allows rapid solvent removal, and drying at room temperature, are necessary to avoid even greater phase separation in the P4VP(A<sub>COOH</sub>)<sub>x</sub> complexes, as found also for similar complexes with another polymer.<sup>26</sup>

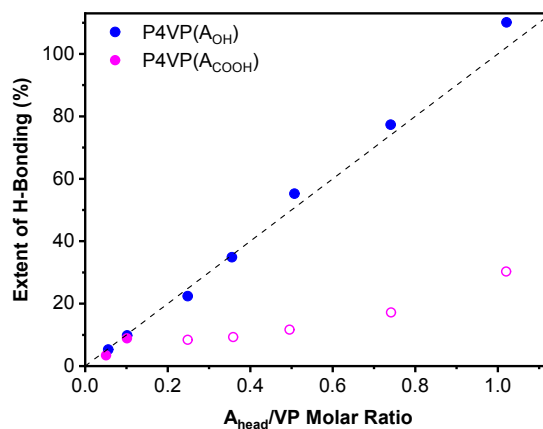


**Fig. 1.** Degree of hydrogen bonding in the P4VP(A<sub>OH</sub>)<sub>x</sub> and P4VP(A<sub>COOH</sub>)<sub>x</sub> complexes. The dashed line represents complete complexation. Closed and open symbols indicate H-bonding of A<sub>head</sub> to P4VP that is complete and partial, respectively.

The UV-visible spectra of the P4VP(A<sub>OH</sub>)<sub>x</sub> system do not show a significant shift of the absorption maximum over the complete range of  $x$ , confirming that the weakly interacting A<sub>OH</sub> chromophores remain unaggregated up to equimolar degrees of complexation (Fig. 2B). This is consistent with the chromophores being completely H-bonded to the polymer, as noted in Fig. 1. In contrast, for both P4VP(A<sub>COOH</sub>)<sub>x</sub> and P4VP(A<sub>CH<sub>3</sub></sub>)<sub>x</sub>, chromophore-chromophore interactions manifest themselves at and above  $x = 0.25$  (Fig. 2A and 2C, respectively), indicative of chromophore crystallization or phase separation. For P4VP(A<sub>COOH</sub>)<sub>0.25-0.50</sub>, the most obvious effect of these interactions is the blue shift of the spectral maxima indicating excitonic coupling (H-aggregation) of two or more adjacent chromophores, suggesting small crystals. For P4VP(A<sub>COOH</sub>)<sub>0.75-1.0</sub>, the spectra are dominated by increased scattering, which can be attributed to macrophase separation of larger crystalline chromophore domains. This type of scattering is evident also in the spectra of the P4VP(A<sub>CH<sub>3</sub></sub>)<sub>x</sub> complexes over the range of  $x = 0.25-1.0$ . At lower  $x$ , it is plausible that most A<sub>CH<sub>3</sub></sub> molecules are dispersed in the P4VP despite the absence of specific

interactions between  $A_{\text{CH}_3}$  and P4VP, as previously observed in mixtures containing up to  $x = 0.08$  of the Disperse Red 1 dye in a non-interacting polystyrene host.<sup>32</sup> Indeed, Fig. 2D shows that for a low  $x$  value of 0.05, the spectrum of P4VP( $A_{\text{CH}_3}$ ) is very similar to that of P4VP( $A_{\text{OH}}$ ), consistent with the similar calculated dipole moments (3.5 and 3.8 D, respectively) of the two chromophores. By contrast, the maximum absorbance in the spectrum of P4VP( $A_{\text{COOH}}$ )<sub>0.05</sub> is red-shifted by  $\sim 25$  nm, consistent with the higher dipole moment of 7.7 D calculated for  $A_{\text{COOH}}$ .

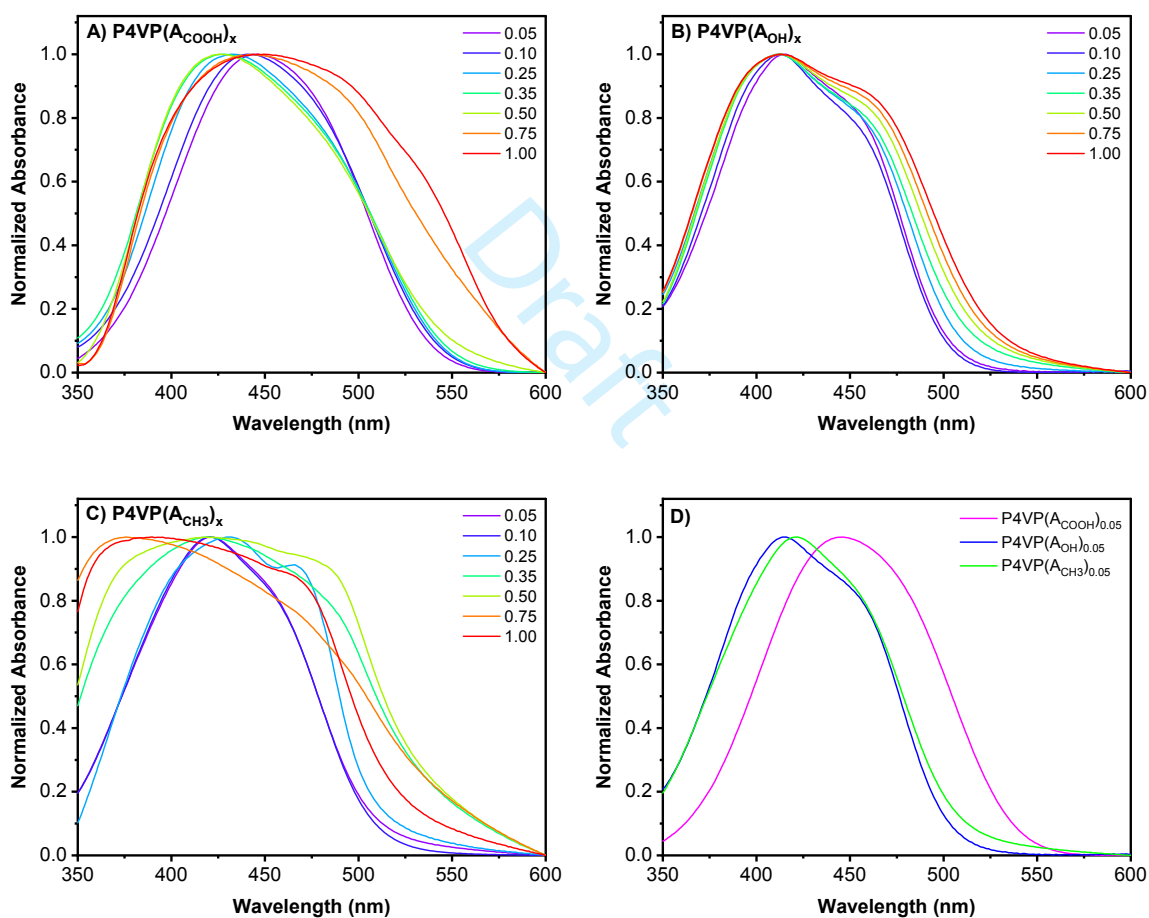


**Fig. 2.** Normalized UV-visible absorption spectra of thin films of A) P4VP( $A_{\text{COOH}}$ )<sub>x</sub>, B) P4VP( $A_{\text{OH}}$ )<sub>x</sub>, and C) P4VP( $A_{\text{CH}_3}$ )<sub>x</sub> for the various  $A_{\text{head}}/\text{VP}$  ratios ( $x$ ) indicated. D) Comparison of the normalized UV-visible absorption spectra of the three systems at  $x = 0.05$ .



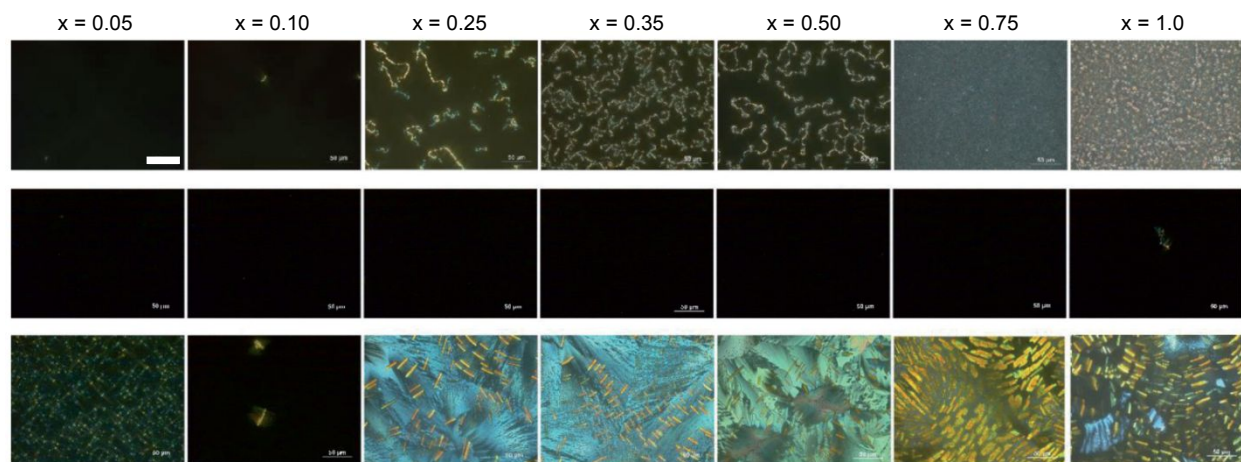


**Fig. 3.** Polarized optical microscopy images for P4VP(A<sub>COOH</sub>)<sub>x</sub> (uppermost line), P4VP(A<sub>OH</sub>)<sub>x</sub> (middle line), and P4VP(A<sub>CH<sub>3</sub></sub>)<sub>x</sub> (bottom line). The scale bar (illustrated in the top left image) is 50 μm for all images.

Additional evidence of crystallization or lack thereof can be observed in the polarized optical microscopy (POM) images of the three systems, illustrated in Fig. 3. The P4VP(A<sub>OH</sub>)<sub>x</sub> samples are non-birefringent – i.e. isotropic – over the whole complexation range investigated, indicating that there is neither phase separation with crystallization of the chromophore (in line with the measured degrees of complexation and the UV-visible spectra) nor liquid crystal character in the complexes, as found also in Ref 33. In contrast, birefringent domains appear in most of the P4VP(A<sub>COOH</sub>)<sub>x</sub> and P4VP(A<sub>CH<sub>3</sub></sub>)<sub>x</sub> samples, which can be related to azo crystallization, in line with the extent of complexation and the UV-visible spectra. The P4VP(A<sub>CH<sub>3</sub></sub>)<sub>x</sub> samples show highly intense and essentially continuous birefringence for  $x = 0.25$  and above. This is consistent with what might be expected for a system with no specific interactions between the chromophore and the polymer, such that extensive and relatively unimpeded crystallization takes place above a low solubility limit that depends on the chemical nature of the azo dye and the polymer matrix. For

P4VP(A<sub>COOH</sub>)<sub>x</sub>, birefringence appears at  $x = 0.25$  in the form of mainly isolated domains whose density tends to increase with increasing  $x$ . In this case, the H-bond interactions of A<sub>COOH</sub> with P4VP, even if at a relatively low level, likely impede azo crystallization and limit crystallite size, thus diminishing the resultant birefringence in POM. It may also be noted that there appears to be a correlation between the blue-shifted UV-visible spectra of P4VP(A<sub>COOH</sub>)<sub>0.25-0.50</sub> and the POM images showing isolated birefringent areas on a dark background, indicating the presence of both optically anisotropic and isotropic domains in these samples, whereas the dominance of scattering effects in the UV-visible spectra of P4VP(A<sub>COOH</sub>)<sub>0.75-1.0</sub> can be related to the greater density of birefringent structures in the POM images.

For what follows, a word should be said about the glass transition temperature ( $T_g$ ). The  $T_g$  of the P4VP used is about 125 °C.<sup>34</sup> The addition of H-bonded azo derivatives generally decreases the  $T_g$  with added azo due to a plasticizing effect which can be followed by an increase in  $T_g$  as full complexation is approached due to decreasing mobility of the highly complexed azos, such that the minimum  $T_g$  reached is roughly 60 °C for azos similar to those used here.<sup>6,26,33-34</sup> Furthermore, in the presence of phase-separated (crystallized) azo, the P4VP  $T_g$  is less affected.<sup>26</sup> We conclude that, because the system  $T_g$  is always well above ambient temperature, it is unlikely that the precise  $T_g$ s of the systems under study have a large effect on the optical properties described below.

Fig. 4 illustrates the order parameter of the chromophores that is reached in the complexes after illumination with linearly polarized 488 nm light. This pump wavelength, which was also used for the SRG inscription experiments, is absorbed by both the trans ( $\pi - \pi^*$  band) and cis ( $n - \pi^*$  band) conformers of all three azobenzene compounds studied. This promotes rapid trans–cis and cis–trans photochemical reactions as is needed for efficient photo-orientation and all-optical

SRG inscription. This light orients the chromophores in the direction perpendicular to the incident polarization, hence giving negative S values. The maximum orientation is obtained at low x for all samples and decreases with increasing x. A similar decrease in azo orientation with increasing x was found for other H-bonded<sup>8</sup> and halogen-bonded<sup>24</sup> azopolymer complexes. However, the trend in the decrease of S is smooth for P4VP(A<sub>OH</sub>) complexes over the whole range of x and tends toward a plateau, analogously to what was observed for saturated photoinduced birefringence normalized by number density of chromophores in this material.<sup>33</sup> In contrast, an abrupt change is observed for P4VP(A<sub>COOH</sub>) above x=0.5, and possibly also for P4VP(A<sub>CH<sub>3</sub></sub>) (although the already low S at x = 0.35-0.5 makes this difficult to see clearly), both of which contain crystallized chromophore at higher x.

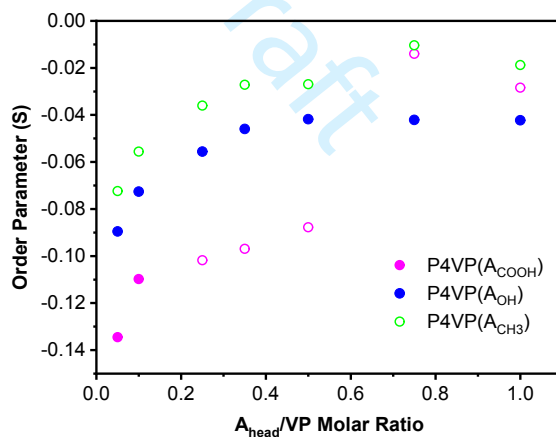


**Fig. 4.** Order parameter after illumination of 300 s with linearly polarized 488 nm light. Open symbols indicate partial crystallization of the azobenzene chromophores.

At low x, where aggregation is minimal or inexistent, the P4VP(A<sub>COOH</sub>) system reaches a substantially higher orientation than P4VP(A<sub>OH</sub>) and P4VP(A<sub>CH<sub>3</sub></sub>). While this partially reflects a tendency of azo compounds with a higher dipole moment to orient more due to more efficient

trans-cis-trans isomerization cycling,<sup>35,36</sup> differences in absorption coefficients of the three chromophores at 488 nm (see Fig. 2D) may also contribute to the higher order parameters reached by  $A_{\text{COOH}}$ . The detrimental effect of chromophore aggregation on photo-orientation is clearly visible in this data, since the orientation values for  $\text{P4VP}(A_{\text{COOH}})_{0.75-1.0}$  become lower than for  $\text{P4VP}(A_{\text{OH}})_{0.75-1.0}$  which forms weaker H-bonds but resists phase separation. Values for  $\text{P4VP}(A_{\text{COOH}})_{0.75-1.0}$  reach the same low orientation level as those for  $\text{P4VP}(A_{\text{CH}_3})_{0.75-1.0}$  having no specific supramolecular interaction with the polymer backbone and thus certainly subject to chromophore-chromophore intermolecular interactions.

Generally, the values of  $S$  do not distinguish between whether the photo-orientation is caused by angular hole burning (AHB) due to polarization-selective azobenzene trans-cis isomerization, by angular redistribution (AR) of the long axis of the trans molecules, or by both.<sup>37,38</sup> More insight can be gained by comparing, as done in Fig. 5, the polarized absorption spectra under irradiation with the spectrum measured in the dark before irradiation. As expected, the parallel-polarized absorbance (full lines) decreases upon irradiation as both AHB and AR processes reduce the number of trans conformers in the direction parallel to the laser polarization. The behaviour of the perpendicular-polarized spectra (dashed lines) is more distinctive. With  $x = 0.05$ , the perpendicular absorbance after 5 min of irradiation is lower than in the original spectrum, and not higher as one would expect if the azobenzene chromophores were simply reoriented under irradiation. A biaxial orientation<sup>39</sup> may partially contribute to this observation but it cannot be the dominating effect because it would imply a very strong tendency to orient in the out-of-plane direction, which is extremely unlikely for an amorphous well-dispersed system. We thus interpret the decreasing perpendicular-polarized absorbance as evidence that angular hole burning is the dominant effect responsible for the  $S$  for all three systems (panels A, D and G of Fig. 5) at low  $x$ . In contrast, at  $x$

= 1.0, the absorbance for P4VP( $A_{\text{COOH}}$ ) becomes larger than the initial value, a clear indication of angular redistribution (Fig. 5C). The relative changes in parallel and perpendicular absorbances compared to the initial spectrum in the dark suggest that the uniaxial model is an appropriate approximation to calculate the S values. After 5 min of relaxation in the dark (not shown), the perpendicular-polarized absorbance further increases due to the reversed AHB process, the cis-trans isomerization. The relative importance of the AR mechanism appears to gradually increase for P4VP( $A_{\text{COOH}}$ )<sub>x</sub> systems of increasing x value, as illustrated in Fig. 5B for P4VP( $A_{\text{COOH}}$ )<sub>0.5</sub>. A similar trend can be noted for P4VP( $A_{\text{OH}}$ )<sub>x</sub>, although the absorbance with perpendicular polarization does not exceed the dark spectrum even for P4VP( $A_{\text{OH}}$ )<sub>1.0</sub>. Because of strong scattering, it is not possible to firmly establish the behaviour of P4VP( $A_{\text{CH}_3}$ )<sub>x</sub> with x = 0.5 or 1.0. These results support our previous observations that stronger chromophore-chromophore interactions promote the angular redistribution mechanism and that its relative importance, compared to AHB, increases at higher azobenzene content.<sup>8</sup> In view of this, the partial aggregation of the chromophores could improve the photoresponse of the system, as it does for liquid-crystalline azopolymers,<sup>7,14</sup> to the extent that the optical properties of the thin films remain acceptable.

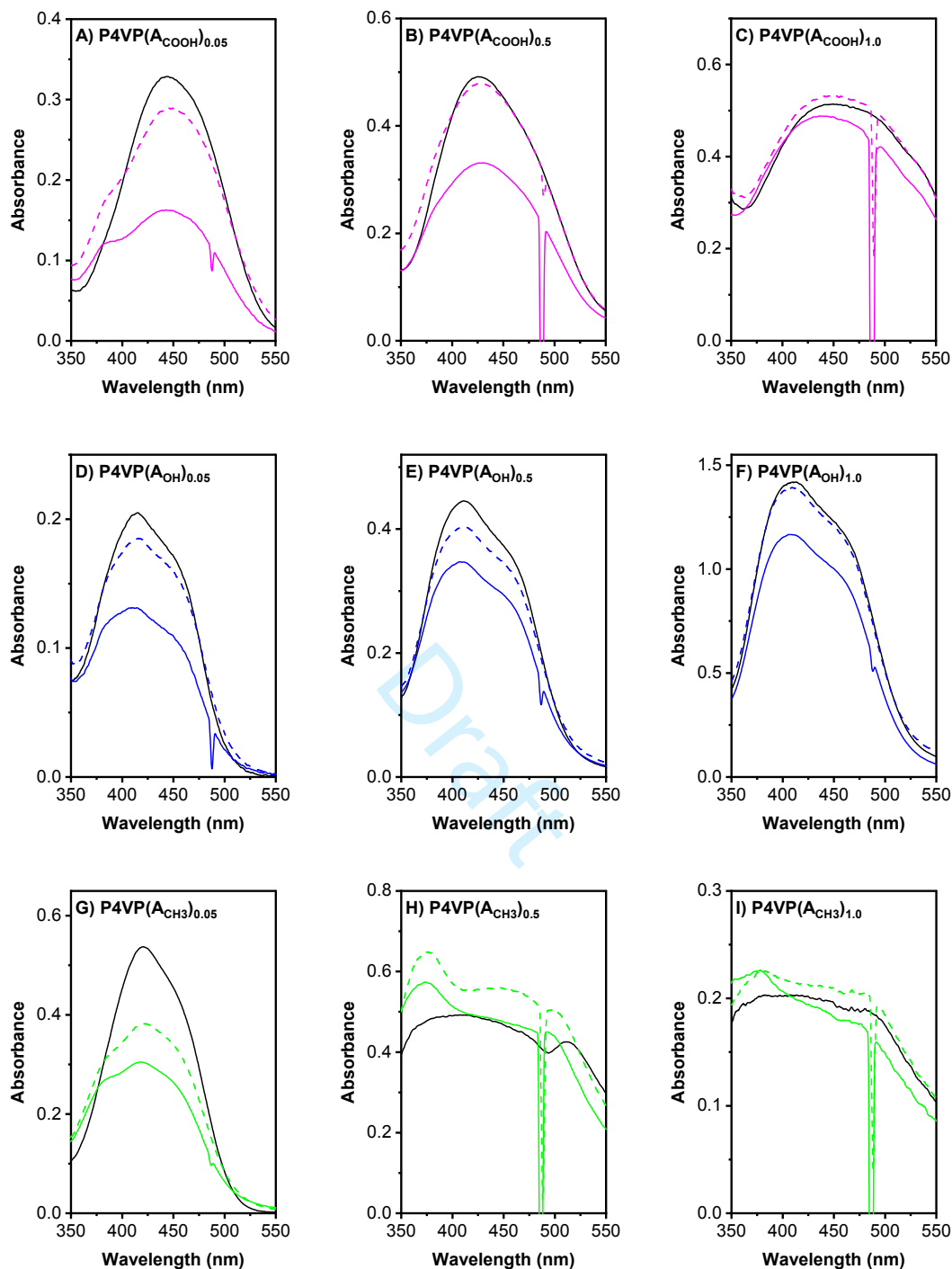


**Fig. 5.** Comparison of the UV-visible spectra polarized parallel and perpendicular to the laser polarization direction (full and dashed lines, respectively) recorded after 5 min of 488 nm laser irradiation. The spectra prior to illumination are shown as black lines. The sharp features at 488 nm are due to stray laser light.

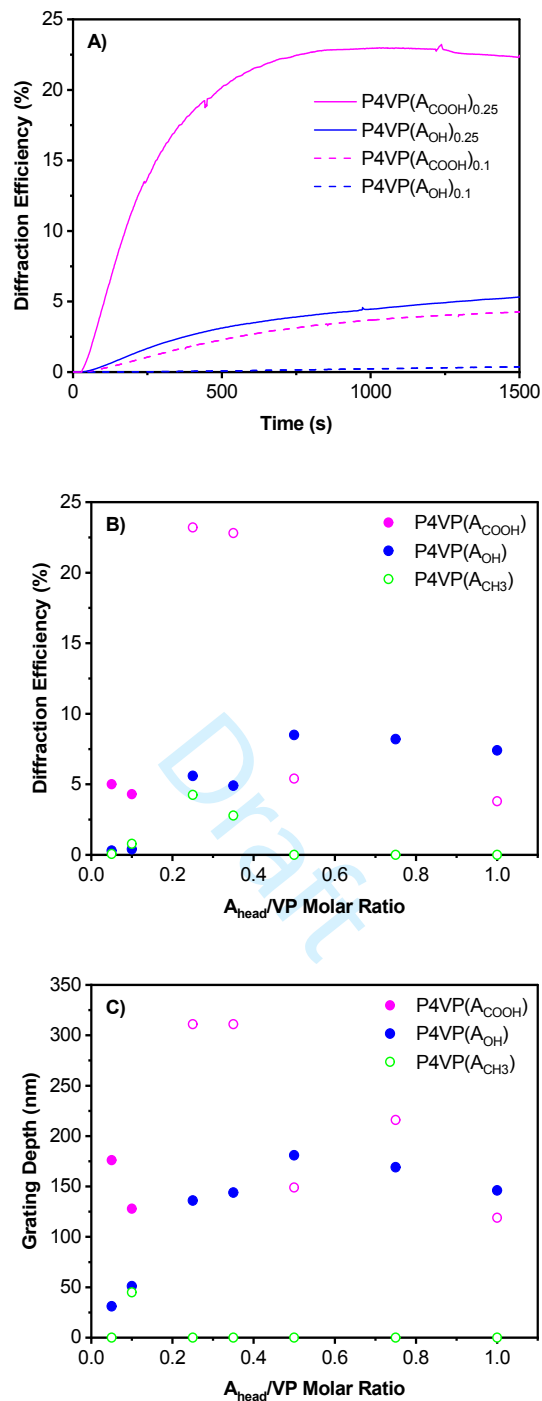


**Fig. 6.** A) Representative SRG inscription curves, B) maximum diffraction efficiency reached upon SRG inscription, and C) the corresponding grating modulation depth measured by AFM. Open symbols indicate crystallization of the azobenzene chromophores.

SRG inscription on thin films of the different samples demonstrates the same interplay of intermolecular interaction strength and molecular structure, as do the absorption and photo-orientation results. Figure 6A illustrates the SRG writing dynamics for P4VP(A<sub>OH</sub>) and P4VP(A<sub>OH</sub>) with  $x = 0.1$ , where the azo is well dispersed in both complexes, and with  $x = 0.25$ , where phase separation has already begun for P4VP(A<sub>COOH</sub>). The diffraction efficiency smoothly increases with time in all cases but at a much faster rate for P4VP(A<sub>COOH</sub>) and with increasing  $x$ . Qualitatively, saturation of the diffraction efficiency is reached within 1500 s only for the P4VP(A<sub>COOH</sub>)<sub>0.25</sub> sample. Figure 6B plots the maximum diffraction efficiency reached by all samples. The most important observation, in terms of our initial objective of comparing the effect of the H-bond strength, is that at low degrees of complexation ( $x = 0.05-0.10$ ), where there is maximal H-bonding with P4VP and no A<sub>COOH</sub> phase separation, the diffraction efficiencies reached are clearly higher for the P4VP(A<sub>COOH</sub>) films than for the P4VP(A<sub>OH</sub>) films. This trend is mirrored in Figure 6C when plotting the *ex-situ* measured modulation depths of the inscribed patterns as determined by AFM. This correlation between H-bond strength and SRG response thus complements the same structure-function relationship observed in halogen-bonded materials<sup>25</sup> and when comparing H-bonded materials with analogous ionically-bonded and mixed H-bonded/ionically bonded materials.<sup>26</sup>

Even for  $x = 0.25$  and  $0.35$ , where A<sub>COOH</sub> H-bonding to P4VP is drastically reduced and A<sub>COOH</sub> crystallization has set in (but keeping in mind that part of the non-bonded A<sub>COOH</sub> probably remains molecularly dispersed within the polymer matrix instead of crystallizing), the P4VP(A<sub>COOH</sub>) films continue to surpass the P4VP(A<sub>OH</sub>) films by about fourfold and twofold, respectively, which may be indicative of a relatively low degree of A<sub>COOH</sub> crystallization at these  $x$ .



It may be noted that the SRG efficiency and grating amplitude tend to increase with increase in molar ratio in the lower  $x$  range, up to about 0.35 for P4VP( $A_{COOH}$ ) and about 0.5 for P4VP( $A_{OH}$ ), this much more strongly for the former than the latter as noted in the previous paragraph. Above  $x = 0.35$ , the response in the P4VP( $A_{COOH}$ ) films is degraded strongly, which can be attributed to significant  $A_{COOH}$  crystallization. In an analogous system, Gao *et al.* also reported an increase in the SRG modulation depth until only  $x = 0.40$ .<sup>9</sup> Despite the degradation in response at higher molar ratios, the measured grating depths in the P4VP( $A_{COOH}$ ) films are similar to those of the P4VP( $A_{OH}$ ) films in the 0.45-1.0 range of  $x$ , although the diffraction efficiencies of the former are a little less. In general, the properties of partially aggregated materials depend on many parameters of the thin film preparation, for instance on the rate of solvent evaporation, which particularly influences the degree of phase separation when this tendency is present.<sup>26,30</sup> Furthermore, the random nature of crystalline nucleation influences final crystalline forms and sizes.

It is noteworthy that the SRG efficiency and amplitude trends for P4VP( $A_{OH}$ ) <sub>$x$</sub>  as a function of degree of complexation (Fig. 6) reach their maximum near  $x = 0.5$  and then remain approximately constant or even decrease a little. This contrasts with what was observed by Vapaavuori *et al.* for the same complexes,<sup>33</sup> where the response tended to increase up to  $x = 1.0$ . On the other hand, a similar trend in SRG efficiency and amplitude as a function of  $x$  was observed in amorphous P4VP-bisazobenzene complexes.<sup>34,40</sup> Some possible explanations are the differences in the interference patterns used to inscribe gratings, since it is known that the inscription depends on the initial polarization<sup>41-43</sup> and might also depend on other experimental parameters, such as film thickness, drying conditions and ambient humidity.

Finally, it is of interest to note that there are measurable diffraction efficiencies in the low molar ratio P4VP(A<sub>CH3</sub>) films, having similar magnitudes to those in P4VP(A<sub>OH</sub>) films for  $x$  up to 0.25 but decreasing to 0 for  $x \geq 0.5$ , suggesting that photoisomerization of the chromophores without specific interactions with the polymer backbone, if (mainly) dispersed in the polymer matrix, is enough to drive SRG formation. On the other hand, only one sample,  $x = 0.1$ , shows a measurable SRG amplitude. Further studies, for instance using different diffraction patterns and benefiting from the recently demonstrated *in-situ* AFM methods,<sup>44,45</sup> are desirable to understand this phenomenon.

## Conclusion

Varying para-substitution of photoactive azobenzene chromophores is a simple way to alter their interaction strength with complementary photopassive polymer matrices. This creates a useful parameter space for studying structure-function relationships of photoinduced motions in azobenzene-containing supramolecular complexes and for optimizing their photoresponse. Overall, the above results indicate that for greater SRG and photo-orientation response in H-bonded azopolymer complexes, it is desirable to use azo derivatives forming stronger H-bonds with the polymer host, while also maintaining maximal H-bonding and amorphous character up to high azo molar ratios. COOH-functionalized derivatives outperform their OH-functionalized analogs when the azo content is sufficiently low to avoid aggregation, since at higher azo content they tend to crystallize due to acid dimerization, leading to a degradation of the optical performance. The acid-functionalized system can still outperform the fully complexed hydroxyl-functionalized system when aggregation is not too pervasive, suggesting that it might be possible to optimize preparation conditions to give partially aggregated functional materials that perform

well. A more promising approach is the molecular design of azobenzene derivatives with a strong H-bond donating functionality where crystallization is inhibited by, for example, a nearby moiety that introduces steric hindrance or irregularity. Such system would combine the key characteristics of maximal complexation and lack of aggregation even at the high azo content needed to produce supramolecular materials with a strong photoresponse using the common H-bond.

## Experimental

### Sample preparation

P4VP ( $M_n = 5100$  g/mol,  $M_w = 5400$  g/mol) was obtained from Polymer Source and the three azo derivatives from Tokyo Chemical Industry; all were used as received. Mixtures of P4VP and  $A_{\text{head}}$  were prepared by dissolving the constituents individually in DMF, filtering the solutions through 0.2  $\mu\text{m}$  PTFE syringe filters, and then mixing them at desired  $A_{\text{head}}:\text{VP}$  molar ratios ( $x$ ). The P4VP( $A_{\text{COOH}}$ ) $_x$  solutions, which tended to precipitate over time, were heated to approximately 90 °C for redissolution just before film preparation. Film samples were prepared by spin-coating (unless otherwise specified, for 60 s at 800-1200 rpm followed by 15 s at 1500 rpm with a 500 rpm/s acceleration), and left to dry in a fumehood at room temperature overnight or longer. Films thicknesses generally varied between 100 and 260 nm for P4VP( $A_{\text{COOH}}$ ) and P4VP( $A_{\text{OH}}$ ), and around 600 nm for P4VP( $A_{\text{CH}_3}$ ).

### Computations

DFT calculations were done using Gaussian 16 on the supercomputer Graham managed by Compute Canada. The dipole moment of the azo chromophores were calculated with the B3LYP functional and the 6-31+G(d,p) basis set. The geometry of the molecules was optimized *in vacuo*.

### Infrared spectroscopy

Samples for FT-IR characterization were prepared by spin-coating 75  $\mu\text{L}$  solutions of P4VP( $A_{\text{head}}$ ) in DMF, with a P4VP concentration of 9–10 wt %, on KBr windows at a speed of 700 rpm for 30 s. The samples were dried at room temperature in the container of an FTS Systems FD-3-85A-MP freeze-dryer equipped with a condenser working at 1–3 mT and  $-90\text{ }^{\circ}\text{C}$  for 2 h followed by at least 3 d in a covered Petri dish in a fumehood. FT-IR measurements were performed in transmission on a Bruker Optics Tensor 27 spectrometer with a HgCdTe detector. All spectra were obtained with a resolution of  $4\text{ cm}^{-1}$  by averaging 512 scans. The fraction of H-bonded pyridines was determined using the procedures described in Wang *et al.*<sup>8</sup>

### UV-visible spectroscopy

Non polarized spectra were recorded with a PerkinElmer Lambda 950 spectrometer. Pure quartz glass was used as a reference. Photo-orientation studies were performed by illuminating the thin films with a 488 nm linearly polarized argon laser. The polarized UV-visible spectra were taken with an Ocean Optics USB2000+ spectrometer before and after 300 s of irradiation. The light incident to the sample was polarized using a broad-band polarizer, which was manually rotated between the two in-plane polarizations. The order parameters,  $S$ , were calculated at the maximum absorbance of each sample using the equation

$$S = \frac{A_{\parallel} - A_{\perp}}{A_{\parallel} + 2A_{\perp}}$$

where  $A_{\parallel}$  and  $A_{\perp}$  are the absorbances parallel and perpendicular to the laser polarization direction, respectively.

### Polarized optical microscopy

To determine the amorphous or anisotropic (crystalline or liquid crystalline) character of the samples, polarized optical microscopy images were obtained with a Leica DM4500P polarized optical microscope.

### Optical grating formation

The surface-relief grating (SRG) formation was studied by measuring the first-order diffraction efficiency of a low-intensity 635 nm non-resonant laser diode from the pattern that was inscribed using a Lloyd's mirror interferometer set-up with an argon laser operating at 488 nm with approximately 200 mW/cm<sup>2</sup> irradiance. The values reported here as the maximum diffraction efficiencies were read after 1500 s of inscription. The resulting surface patterns were characterized by *ex-situ* atomic force microscopy (AFM) measurements carried out using a Veeco Dimension 5000 SPM in tapping mode.

### Acknowledgements

CP and CGB acknowledge funding by the Natural Sciences and Engineering Research Council (NSERC; grants RGP/77200073-2014 and RGPIN/04014-2015) of Canada. JV was supported by postdoctoral fellowships from the Academy of Finland and the Banting program (Canada). AP acknowledges the financial support of the Academy of Finland (decision numbers 277091 and 312628).

### References

- (1) Vapaavuori, J.; Bazuin, C. G.; Priimagi, A. *J. Mater. Chem. C* **2018**, *6*, 2168, doi:10.1039/C7TC05005D.
- (2) Faul, C. F. J. *Acc. Chem. Res.* **2014**, *47* (12), 3428, doi:10.1021/ar500162a.
- (3) Stumpe, J.; Kulikovska, O.; Goldenberg, L. M.; Zakrevskyy Z., pp. 47–94. In *Smart Light-Responsive Materials*; Ikeda, Y. Z. and T., Ed.; John Wiley & Sons Ltd.: Hoboken, NJ,

- USA, 2009.
- (4) Hofman, A. H.; ten Brinke, G.; Loos, K. *Polymer*, **2016**, *107*, 343, doi:10.1016/j.polymer.2016.08.021.
- (5) Ten Brinke, G.; Ikkala, O. *Chem. Rec.* **2004**, *4*, 219, doi:10.1002/tcr.20018.
- (6) Priimagi, A.; Vapaavuori, J.; Rodriguez, F. J.; Faul, F. J.; Heino, M. T.; Ikkala, O.; Kauranen, M.; Kaivola, M. *Chem. Mater.* **2008**, *20*, 6358, doi:10.1021/cm800908m.
- (7) Zhang, Q.; Bazuin, C. G.; Barrett, C. J.; *Chem. Mater.* **2008**, *20*, 29, doi:10.1021/cm702525y.
- (8) Wang, X.; Vapaavuori, J.; Bazuin, C. G.; Pellerin, C. *Macromolecules* **2018**, *51*, 1077, doi:10.1021/acs.macromol.7b02534.
- (9) Gao, J.; He, Y.; Liu, F.; Zhang, X.; Wang, Z.; Wang, X. *Chem. Mater.* **2007**, *19*, 3877, doi:10.1021/cm0707197.
- (10) Schab-Balcerzak, E.; Flakus, H.; Jarczyk-Jedryka, A.; Konieczkowska, J.; Siwy, M.; Bijak, K.; Sobolewska, A.; Stumpe, J. *Opt. Mater.* **2015**, *47*, 501, doi:10.1016/j.optmat.2015.06.029.
- (11) Wu, S.; Duan, S.; Lei, Z.; Su, W.; Zhang, Z.; Wang, K.; Zhang, Q. *J. Mater. Chem.* **2010**, *20*, 5202, doi:10.1039/c000073f.
- (12) Del Barrio, J.; Blasco, E.; Toprakcioglu, C.; Koutsioubas, A.; Scherman, O. A.; Oriol, L.; Sánchez-Somolinos, C. *Macromolecules* **2014**, *47*, 897, doi:10.1021/ma402369p.
- (13) Konieczkowska, J.; Wojtowicz, M.; Sobolewska, A.; Noga, J.; Jarczyk-Jedryka, A.; Kozanecka-Szmigiel, A.; Schab-Balcerzak, E. *Opt. Mater.* **2015**, *48*, 139, doi:10.1016/j.optmat.2015.07.033.
- (14) Zhang, Q.; Wang, X.; Barrett, C. J.; Bazuin, C. G. *Chem. Mater.* **2009**, *21*, 3216,

- doi:10.1021/cm900810r.
- (15) Natansohn, A.; Rochon, P. *Chem. Rev.* **2002**, *102*, 4139, doi:10.1021/cr970155y.
- (16) Priimagi, A.; Shevchenko, A. *J. Polym. Sci. Part B Polym. Phys.* **2014**, *52*, 163, doi:10.1002/polb.23390.
- (17) Seki, T. *Macromol. Rapid Commun.* **2014**, *35*, 271, doi:10.1002/marc.201300763.
- (18) Mahimwalla, Z.; Yager, K. G.; Mamiya, J.; Shishido, A.; Priimagi, A.; Barrett, C. J. *Polym. Bull.* **2012**, *69*, 967, doi:10.1007/s00289-012-0792-0.
- (19) Hendrikx, M.; Schenning, A. P. H. J.; Debije, M. G.; Broer, D. J. *Crystals* **2017**, *7*, 1, doi:10.3390/cryst7080231.
- (20) Lee, S.; Kang, H. S.; Park, J.-K. *Adv. Mater.* **2012**, *24*, 2069, doi:10.1002/adma.201104826.
- (21) Oscurato, S. L.; Salvatore, M.; Maddalena, P.; Ambrosio, A. *Nanophotonics* **2018**, *7*, 1387, doi:10.1515/nanoph-2018-0040.
- (22) Kim, K.; Park, H.; Park, K. J.; Park, S. H.; Kim, H. H.; Lee, S. *Adv. Opt. Mater.* **2019**, *7*, 1900074, doi:10.1002/adom.201900074.
- (23) Vapaavuori, J.; Siiskonen, A.; Dichiarante, V.; Forni, A.; Saccone, M.; Pilati, T.; Pellerin, C.; Shishido, A.; Metrangolo, P.; Priimagi, A. *RSC Adv.* **2017**, *7*, 40237, doi:10.1039/c7ra06397k.
- (24) Vapaavuori, J.; Heikkinen, I. T. S.; Dichiarante, V.; Resnati, G.; Metrangolo, P.; Sabat, R. G.; Bazuin, C. G.; Priimagi, A.; Pellerin, C. *Macromolecules* **2015**, *48*, 7535, doi:10.1021/acs.macromol.5b01813.
- (25) Saccone, M.; Dichiarante, V.; Forni, A.; Goulet-Hanssens, A.; Cavallo, G.; Vapaavuori, J.; Terraneo, G.; Barrett, C. J.; Resnati, G.; Metrangolo, P.; Priimagi, A. *J. Mater. Chem.*

- C* **2015**, *3*, 759, doi:10.1039/c4tc02315c.
- (26) Wang, X.; Vapaavuori, J.; Wang, X.; Sabat, R. G.; Pellerin, C.; Bazuin, C. G. *Macromolecules* **2016**, *49*, 4923, doi:10.1021/acs.macromol.6b01009.
- (27) Roland, S.; Gaspard, D.; Prud'homme, R. E.; Bazuin, C. G. *Macromolecules* **2012**, *45*, 5463, doi:10.1021/ma3007398.
- (28) Lee, J.; Painter, P.; Coleman, M. *Macromolecules* **1988**, *21*, 954, doi:10.1021/ma00182a019.
- (29) Wu, S.; Bubeck, C. *Macromolecules* **2013**, *46*, 3512, doi:10.1021/ma400104d.
- (30) Brandys, F. A.; Bazuin, C. G. *Chem. Mater.* **1996**, *8*, 83, doi:10.1021/cm950240r.
- (31) Koskela, J. E.; Vapaavuori, J.; Ras, R. H. A.; Priimagi, A. *ACS Macro Lett.* **2014**, *3*, 1196, doi:10.1021/mz500616q.
- (32) Priimagi, A.; Cattaneo, S.; Ras, R. H. A.; Valkama, S.; Ikkala, O.; Kauranen, M. *Chem. Mater.* **2005**, *17*, 5798, doi:10.1021/cm051103p.
- (33) Vapaavuori, J.; Valtavirta, V.; Alasaarela, T.; Mamiya, J.-I.; Priimagi, A.; Shishido, A.; Kaivola, M. *J. Mater. Chem.* **2011**, *21*, 15437, doi:10.1039/c1jm12642c.
- (34) Vapaavuori, J.; Priimagi, A.; Kaivola, M. *J. Mater. Chem.* **2010**, *20*, 5260, doi:10.1039/c0jm00021c.
- (35) Brown, D.; Natansohn, A.; Rochon, P. *Macromolecules* **1995**, *28*, 6116, doi:10.1021/ma00122a019.
- (36) Natansohn, A.; Rochon, P.; Ho, M. S.; Barrett, C. *Macromolecules* **1995**, *28*, 4179, doi:10.1021/ma00116a019.
- (37) Blanche, P.-A.; Lemaire, P. C.; Dumont, M.; Fischer, M. *Opt. Lett.* **1999**, *24*, 1349, doi:10.1364/ol.24.001349.



- (38) Dumont, M. L.; Sekkat, Z *Proc. SPIE* **1993**, *1774*, 188, doi:10.1117/12.139169.
- (39) Buffeteau, T.; Lagugné Labarthe, F.; Sourisseau, C.; Kostromine, S.; Bieringer, T.; *Macromolecules* **2004**, *37*, 2880, doi: 10.1021/ma030471g.
- (40) Koskela, J. E.; Vapaavuori, J.; Hautala, J.; Priimagi, A.; Faul, C. F. J.; Kaivola, M.; Ras, R. H. A. *J. Phys. Chem. C* **2012**, *116*, 2363, doi:10.1021/jp210706n.
- (41) Viswanathan, N. K.; Balasubramanian, S.; Li, L.; Tripathy, S. K.; Kumar, J. A *Japanese J. Appl. Physics* **1999**, *38*, 5928, doi:10.1143/jjap.38.5928.
- (42) Audorff, H.; Walker, R.; Kador, L.; Schmidt, H. W. *J. Phys. Chem. B* **2009**, *113*, 3379, doi:10.1021/jp809151x.
- (43) Yadavalli, N. S.; Saphiannikova, M.; Santer, S. *Appl. Phys. Lett.* **2014**, *105*, 051601, doi:10.1063/1.4891615.
- (44) Yadavalli, N. S.; Santer, S. *J. Appl. Phys.* **2013**, *113*, 224304, doi:10.1063/1.4809640.
- (45) Jelken, J.; Santer, S *RSC Adv.* **2019**, *9*, 20295, doi:10.1039/c9ra02571e.

## Figure captions

**Scheme 1.** Chemical structures and nomenclature of the polymer and chromophores used.

**Fig. 1.** Degree of hydrogen bonding in the P4VP(A<sub>OH</sub>)<sub>x</sub> and P4VP(A<sub>COOH</sub>)<sub>x</sub> complexes. The dashed line represents complete complexation. Closed and open symbols indicate H-bonding of A<sub>head</sub> to P4VP that is complete and partial, respectively.

**Fig. 2.** Normalized UV-visible absorption spectra of thin films of A) P4VP(A<sub>COOH</sub>)<sub>x</sub>, B) P4VP(A<sub>OH</sub>)<sub>x</sub>, and C) P4VP(A<sub>CH<sub>3</sub></sub>)<sub>x</sub> for the various A<sub>head</sub>/VP ratios (x) indicated. D) Comparison of the normalized UV-visible absorption spectra of the three systems at x = 0.05.

**Fig. 3.** Polarized optical microscopy images for P4VP(A<sub>COOH</sub>)<sub>x</sub> (uppermost line), P4VP(A<sub>OH</sub>)<sub>x</sub> (middle line), and P4VP(A<sub>CH<sub>3</sub></sub>)<sub>x</sub> (bottom line). The scale bar (illustrated in the top left image) is 50 μm for all images.

**Fig. 4.** Order parameter after illumination of 300 s with linearly polarized 488 nm light. Open symbols indicate partial crystallization of the azobenzene chromophores.

**Fig. 5.** Comparison of the UV-visible spectra polarized parallel and perpendicular to the laser polarization direction (full and dashed lines, respectively) recorded after 5 min of 488 nm laser irradiation. The spectra prior to illumination are shown as black lines. The sharp features at 488 nm are due to stray laser light.

**Fig. 6.** A) Representative SRG inscription curves, B) maximum diffraction efficiency reached upon SRG inscription, and C) the corresponding grating modulation depth measured by AFM. Open symbols indicate crystallization of the azobenzene chromophores.